

Low temperature processing of interlayer-free $\text{La}_{0.6}\text{Sr}_{0.4}\text{Co}_{0.2}\text{Fe}_{0.8}\text{O}_{3-\delta}$ cathodes for intermediate temperature solid oxide fuel cells

Ze Lei ^{a,b}, Qingshan Zhu ^{a,*}, Li Zhao ^{a,b}

^a Multiphase Reaction Laboratory, Institute of Process Engineering, Chinese Academy of Sciences, Beijing 100080, China

^b Graduate School of Chinese Academy of Sciences, Beijing 100039, China

Received 13 May 2006; received in revised form 7 June 2006; accepted 8 June 2006

Available online 27 July 2006

Abstract

Nanocrystalline $\text{La}_{0.6}\text{Sr}_{0.4}\text{Co}_{0.2}\text{Fe}_{0.8}\text{O}_{3-\delta}$ (LSCF) powder with a specific surface area of $22.9 \text{ m}^2 \text{ g}^{-1}$ and an average particle size of 175 nm was prepared by a nitrate-glycine solution combustion method and subsequent ball-milling. The LSCF precalcined at 800°C (LSCF-800) shows very good low-temperature sintering activity, and can well adhere to electrolyte after sintering at 700°C and above. The single cell Ni-YSZ/YSZ/LSCF-800 with the cathode sintered at 750°C demonstrates the lowest polarization resistance and good electrical generation performance, but poor cathode microstructure stability. The sintering activity of LSCF cathode can be tailored through the control of the precalcination temperature of the precursor powder. Precalcining of LSCF powder at 900°C (LSCF-900) increases the optimum sintering temperature of the cathode to 850°C and improves the microstructure stability. The cell Ni-YSZ/YSZ/LSCF-900 with this cathode demonstrates excellent generation performances with the maximum power density greater than 1.0 W cm^{-2} and the power density of above 0.80 W cm^{-2} at 0.7 V under operation at 700°C . Low temperature processing of the interlayer-free LSCF cathode with good microstructure is beneficial to simplifying the cell structure and improving fuel cell performance.

© 2006 Elsevier B.V. All rights reserved.

Keywords: Solid oxide fuel cells; LSCF; YSZ; Cathode; Solution combustion method

1. Introduction

Solid oxide fuel cells (SOFCs) have been promising for electrical power generation due to their high-energy conversion efficiency, low pollution emissions and high flexibility to various fuels. Recently, much attention has been focused on lowering the operation temperature to intermediate temperatures ($600\text{--}800^\circ\text{C}$) in order to meet various application requirements, such as facilitating the use of cheap materials and improving the long-term stability [1–3]. Among various cell structures, NiO–8 mol% Y_2O_3 -stabilized ZrO_2 (8YSZ) anode-supported SOFC with a thin zirconia-based electrolyte and a $\text{La}_{1-x-y}\text{Sr}_x\text{O}_{3-\delta}$ (LSM)–YSZ composite cathode is most widely used because of its excellent mechanical reliability and stability in the reduced and oxidized atmospheres (RedOx) cycle [4,5]. However, in the intermediate temperature range, the cathode

overpotential grows significantly and becomes the main issue affecting the cell performance [3,6].

Electron-ion mixed conductor $\text{La}_{0.6}\text{Sr}_{0.4}\text{Co}_{0.2}\text{Fe}_{0.8}\text{O}_{3-\delta}$ (LSCF) possessing high conductivity in air at intermediate temperatures and high catalytic activity for the cathodic reaction is known to be one of the best alternatives to the LSM–YSZ cathode material for intermediate temperature SOFCs (IT-SOFCs). Conventionally, a temperature over 900°C is required for the LSCF cathode fabrication in order to obtain sufficient contact with electrolytes [7]. Unfortunately, solid-state reactions occur between the LSCF cathode and zirconia-based electrolytes above 900°C , and insulating zirconate phases such as SrZrO_3 are often formed at the cathode-electrolyte interface during sintering [7–10]. Thus, a buffer interlayer of doped ceria film such as $\text{Ce}_{0.8}\text{Gd}_{0.2}\text{O}_{2-\delta}$ (CGO) is commonly applied to avoid the deleterious reactions, resulting in the complexity of the cell structure and the manufacturing process. Recently, LSCF cathode prepared from a citrate method was directly applied on the NiO–YSZ anode-supported YSZ electrolyte without interlayer by sintering the cathode below 900°C , suggesting that

* Corresponding author. Tel.: +86 10 62536108; fax: +86 10 62536108.
E-mail address: qs Zhu@home.ipe.ac.cn (Q. Zhu).

LSCF cathodes could be directly utilized on the zirconia-based electrolyte [11]. The performances of SOFCs with LSCF cathodes strongly depend on the powder preparation conditions and resulting microstructure of cathodes [10]. Therefore, through optimizing the processing conditions of the precursor LSCF powder and the resulting microstructure of the cathode, the performance of the cell without the ceria interlayer can be further improved.

In this study, LSCF powders with high sintering activity were synthesized via a nitrate-glycine solution combustion (SC) route, and the sintering activity of LSCF cathode was tailored through the control of the precalcination temperature of the precursor powder. The Ni-YSZ/YSZ/LSCF cell performance was improved through optimizing the sintering procedure and the resulting microstructure of the LSCF cathode.

2. Experimental

2.1. Powder preparation and characterization

LSCF precursor powder was prepared via a solution combustion (SC) route by using nitrates of each element (analytical reagent grade, Beijing Chem. Reag. Co., China) and glycine ($\text{NH}_2\text{CH}_2\text{COOH}$, biological reagent grade, Beijing Aoboxing BioTechnologies Co. Ltd., China) as the starting materials. A mixed solution containing glycine and nitrates (molar ratio of 2.5:1) was heated and concentrated in a big glass beaker at 80°C until it turned to a viscous liquid. The viscous liquid was then heated to $\sim 180^\circ\text{C}$ until spontaneous ignition of the liquid, after which a porous, foamy and fragile material was obtained. The as-ignited material was calcined at 800°C for 5 h in air to remove carbonaceous residues and to form a well crystalline structure, followed by ball-milling at 760 rpm in ethanol for 24 h and drying at 80°C for 24 h (LSCF-800). The phase structure of the LSCF powders was analyzed by an X-ray diffractometer (X'Pert MPD Pro, PANalytical, The Netherlands). The microstructure, particle size distribution and specific surface areas of the powders were characterized by field-emission scanning electron microscopy (FESEM, JSM-6700F, JEOL, Japan), the dynamic laser scattering (DLS) method (90 Plus, BROOKHAVEN, USA) and the BET method (Autosorb-1, QUANTACHROM, USA), respectively.

2.2. Cell fabrication and evaluation of the cathode performance

The 8YSZ powder ($d_{50} = 200$ nm, Jifang Gaotai material Co. Ltd., Shanghai, China) was mixed with NiO powder (Pinggu Shuangyan Chem. Plant, Beijing, China) in weight ratio of 44:56 by ball-milling to form an anode powder mixture, which was subsequently cold-pressed at 50 MPa to form green substrates of 20 mm in diameter and 1 mm in thickness. The green anode substrates were then presintered at 800°C for 4 h. 8YSZ electrolyte film was dip-coated onto the presintered substrates with the slurry consisting of 8YSZ powder, ethanol, ethyl cellulose, and abietyl alcohol. The anode-electrolyte bi-layer was then dried at room temperature, calcined at 350°C for 2 h to remove

the organics, followed by sintering at 1260°C for 2 h. A slurry consisting of LSCF-800 powder, ethyl cellulose and abietyl alcohol was screen-printed onto the electrolyte to form a sandwich of NiO-YSZ/YSZ/LSCF. The sandwich was dried at 80°C for 12 h, then calcined at 350°C for 2 h to remove the organics and sintered at temperatures from 700 to 850°C for 2 h with a heating rate of 1°C min^{-1} . The microstructure of the cathodes was observed by FESEM. Platinum paste and silver paste were screen-printed respectively on the cathode and anode as the current collector.

Single cells were tested at 650 and 700°C in a home-developed-cell-testing system with dry hydrogen as the fuel and static air as the oxidant. The I - V characteristics of the cell were then measured at a constant fuel flow rate of $40\text{ cm}^3\text{ min}^{-1}$ (room temperature). Resistances of the single cells under open circuit conditions were measured using AC impedance spectroscopy (PM6306, Fluke, USA). FESEM was used to reveal the post-test microstructure of the single cell.

3. Results and discussion

3.1. Properties of LSCF powders

Fig. 1 shows the XRD patterns of the LSCF powders calcined at different temperatures. The as-ignited LSCF powder is mainly in the rhombohedral perovskite structure, and only a trace of other phases can be detected. However, after calcination at 800 or 900°C for 5 h, well crystalline LSCF powders with the rhombohedral perovskite structure are obtained. Crystallite sizes calculated according to the Scherrer equation [12] are ~ 25 and 42 nm for the powders calcined at 800 and 900°C for 5 h, respectively. Typical morphologies of the as-calcined LSCF powder and the powder after ball-milling are shown in Fig. 2. It indicates that the as-calcined LSCF powder is porous with foam-like nature, and can be ball-milled to fine particles. The measured surface area of the LSCF powder increases from 11.9 to $22.9\text{ m}^2\text{ g}^{-1}$ after the ball-milling, which is much higher than those prepared by other methods, for instance, a specific surface area of $8.9\text{ m}^2\text{ g}^{-1}$ was reported for the LSCF powder by a citrate method [11]. Dynamic laser scat-

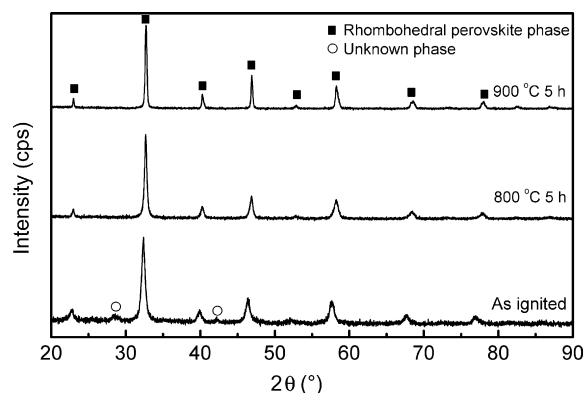


Fig. 1. XRD patterns of the as-ignited LSCF powder and the powders calcined at different temperatures.

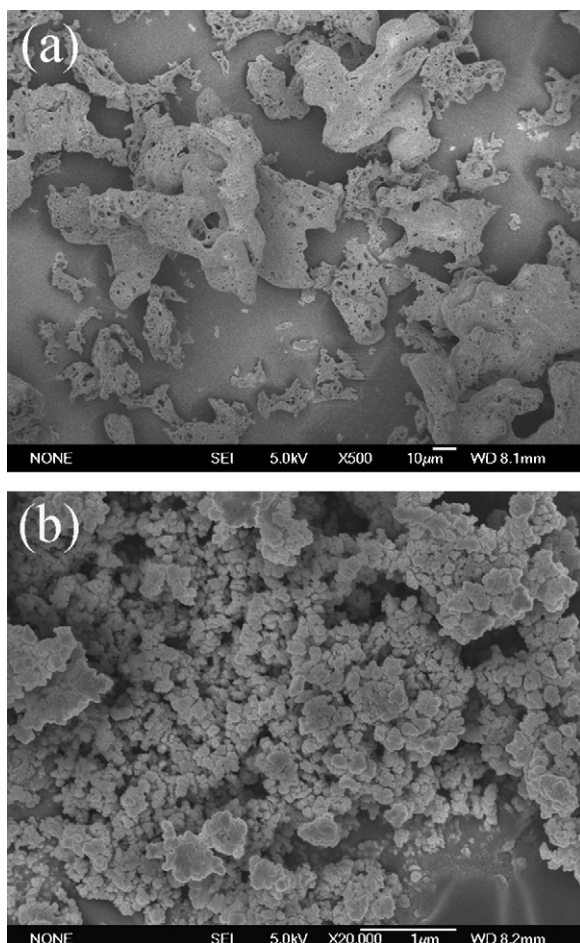


Fig. 2. FESEM micrographs of the LSCF powders calcined at 800 °C for 5h (a) and the powder after subsequent ball-milling at 760 rpm for 24 h (b).

tering investigations reveal that LSCF-800 particles in ethanol exhibit bimodal size distribution with the most probable agglomerate sizes of 26 and 191 nm, as illustrated in Fig. 3. The average agglomerate size is calculated to be 175 nm and 95 vol.% of the agglomerates are in the narrow range of 130–250 nm (Fig. 3), in accordance with the FESEM observation shown in Fig. 2(b).

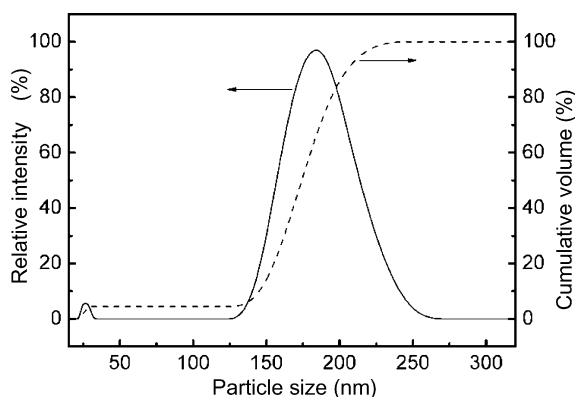


Fig. 3. Particle size distribution of the LSCF-800 powder determined by dynamic laser scattering.

3.2. Sintering behavior of LSCF-800 cathode

Fig. 4 shows the FESEM images of the fractured cross sections of LSCF-800 films on the YSZ electrolyte sintered at temperatures from 700 to 850 °C. It is observed that the nanocrystalline LSCF-800 powder shows high sintering activity, and can be tightly sintered to the dense YSZ electrolyte after sintering at 700 °C or above. The porosity of the cathode decreases with increasing the sintering temperature. Below 850 °C, the cathode has quite uniform structure with an evenly distributed pores of nanometer or submicrometer sizes and good particle-to-particle contact, while at 850 °C or above, nonuniform cathode structure with a denser outer surface, as illustrated by Fig. 4(d), is normally obtained, suggesting that the cathode should be fabricated below 850 °C. The high sintering activity at low temperature achieved in this study is mainly attributed to the small particle size with high surface area and weak agglomeration of precursor powder with narrow particle size distribution. The cathode fabrication temperature below 900 °C would be beneficial to avoid adverse interactions between the LSCF cathode and the zirconia based electrolyte during the NiO–YSZ/YSZ/LSCF fabrication without the ceria interlayer.

3.3. Performances of anode-supported single cells with LSCF-800 cathode

The electric generation performances of the single cell Ni–YSZ/YSZ/LSCF-800 with the cathodes sintered at 700, 750, 800 and 850 °C for 2 h, measured at 650 and 700 °C, are shown in Fig. 5. As can be seen, the performance of the single cell is strongly dependent on the sintering temperature of the cathode. The cell with the cathode sintered at 750 °C has the best performance with the peak-power (mW cm^{-2})/power (mW cm^{-2}) at 0.7 V of 507/390 at 650 °C and 1114/932 at 700 °C, respectively, which is much higher than that reported by Murata et al. for the Ni–YSZ/YSZ/LSCF single cell [11], and the performance is also slightly better than that of the single cell with the CGO interlayer [13], indicating that the electrode performances are sensitive to the preparation conditions of precursor powders. Table 1 summarizes the power densities, the area-specific resistances (ASRs) and ohmic resistances of single cells with LSCF-800 cathodes sintered at various temperatures. The ASRs were calculated by the cell voltage difference between open circuit and at a current density of 1.0 A cm^{-2} according to the literature [2,14], and the ohmic resistances were determined from the high-frequency intercepts of electrochemical impedance spectra. The total polarization resistance of electrodes, including anode and cathode as a function of cathode sintering temperature determined from the difference between the ASR and the ohmic resistance, is plotted in Fig. 6. The lowest polarization resistance is found for the cathode sintered at 750 °C, in accordance with the results of the I – V measurements. It should be noted that the anodes were manufactured under identical conditions, so the difference in the polarization resistance is mainly caused by the cathodes. In general, electrode reactions are closely dependent on the electrode microstructure. The high polarization resistance of the cathode sintered at 700 °C may be attributed to insufficient sintering of

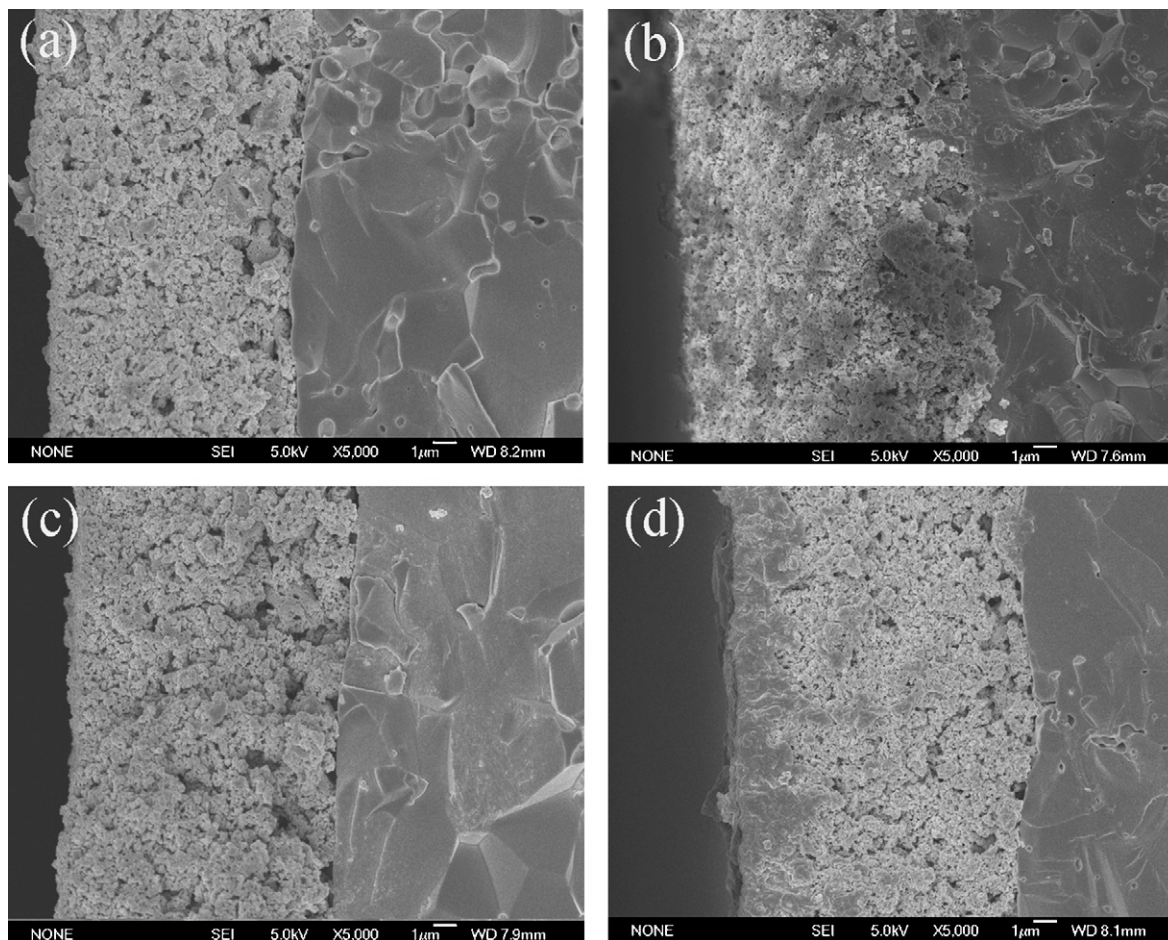


Fig. 4. FESEM photographs of the cross section of LSCF-800 cathode film on the 8YSZ electrolyte sintered at 700 °C (a), 750 °C (b), 800 °C (c) and 850 °C (d) for 2 h.

the cathode, while the high resistance of the cathode sintered at 800 °C or above might be attributed to the over sintering of the cathode that causes the decrease of reactive sites especially on the exterior region, as illustrated by the cross-section in Fig. 4(d).

3.4. Microstructure stability improvement and performance of an anode-supported single cell with LSCF-900 cathode

Since the cathode fabrication temperature is quite close to the cell operation temperature (e.g. 750 °C versus 700 °C), den-

sification of the cathode may proceed during the long term operation at 700 °C. The LSCF-800 cathode fabricated at 750 °C was therefore aged at 700 °C for 100 h to check whether significant microstructure change would occur after the aging test. As shown by the cross section microstructure in Fig. 7(a), significant densification is clearly observed after the aging test, as compared with the microstructure before aging in Fig. 4(b), indicating that the fabrication temperature of 750 °C would be too low to obtain a stabilized cathode for a cell intended to operate at 700 °C. Moreover, serious deterioration of the I - V performance was observed on the cell Ni-YSZ/YSZ/LSCF-

Table 1
Performance of the single cell Ni-YSZ/YSZ/LSCF-800 with LSCF-800 cathode sintered at different temperatures, measured at 650 and 700 °C

Sintering temperature of cathode (°C)	Peak power density (mW cm ⁻²)		Power density at 0.7 V (mW cm ⁻²)		ASR at 1 A cm ⁻² (Ω cm ²) ^a		Ohmic resistance (Ω cm ²) ^b	
	650 °C	700 °C	650 °C	700 °C	650 °C	700 °C	650 °C	700 °C
700	315	825	196	592	0.87	0.34	0.20	0.12
750	507	1114	390	932	0.55	0.24	0.12	0.08
800	360	967	248	834	0.69	0.32	0.15	0.10
850	330	832	243	730	0.73	0.33	0.16	0.11

^a The values were determined by the cell voltage difference between open circuit and at a current density of 1.0 A cm⁻².

^b The values were determined by the high-frequency intercepts in Cole-Cole plots of AC impedance.

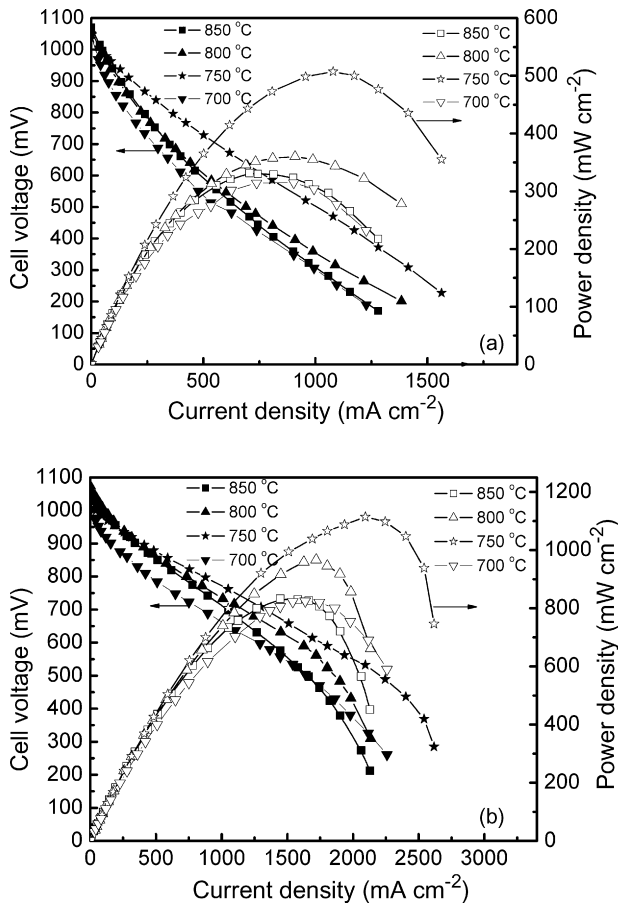


Fig. 5. Cell performance data of anode-supported single cells with LSCF-800 cathode sintered at different temperatures for 2 h, measured at 650 °C (a) and 700 °C (b).

800 after aging at 700 °C for 100 h, in accordance with the fact of the densification of the cathode. These investigations show clearly that the sintering activity of the LSCF-800 should be reduced and a compromise between good cell performance and stable microstructure should be balanced carefully. In the present study, the sintering activity of the LSCF powder is tailored through controlling the calcination temperature, as pow-

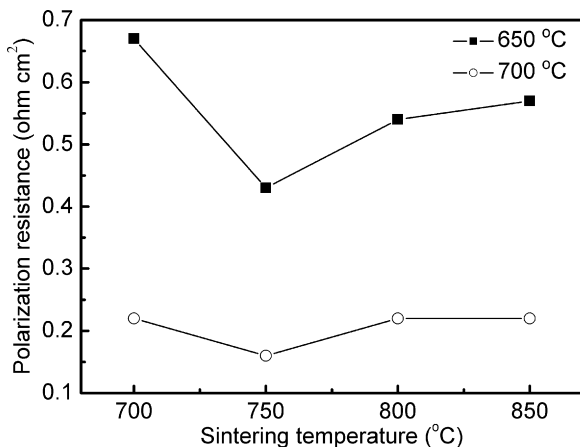


Fig. 6. Polarization resistance of electrodes at various sintering temperature measured at 650 and 700 °C.

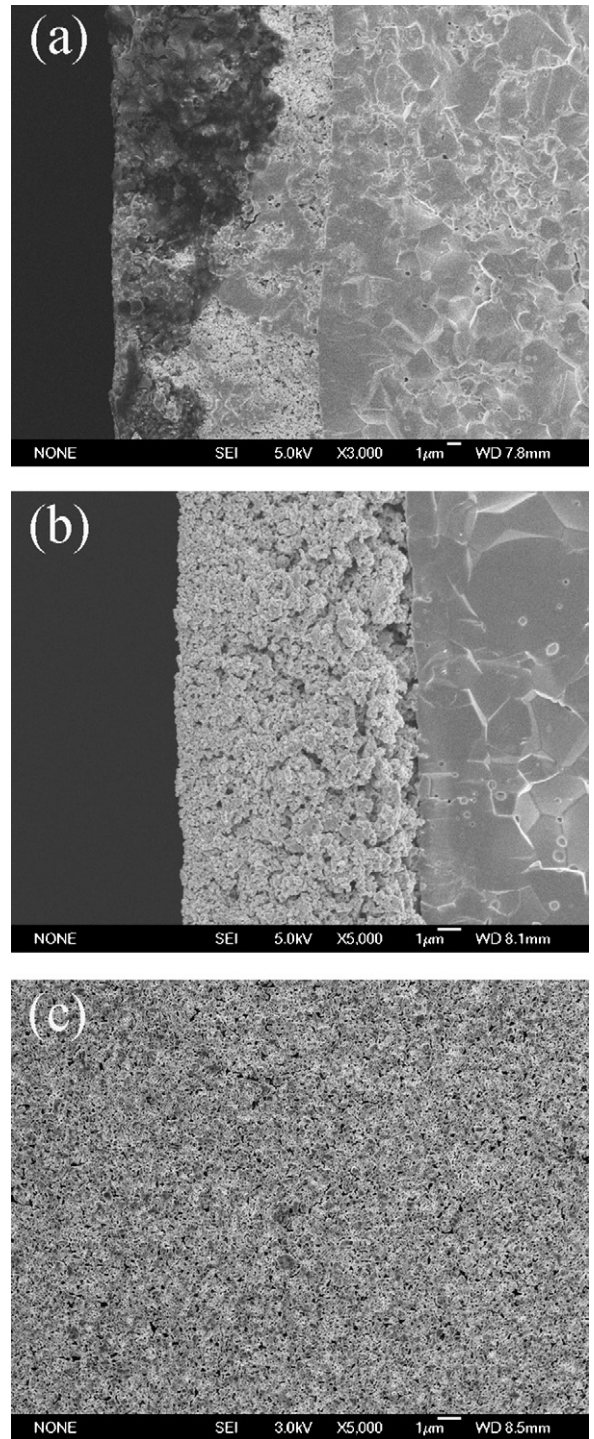


Fig. 7. FESEM images of the fractured cross-section for the samples after aging at 700 °C for 100 h with LSCF-800 cathode on YSZ electrolyte sintered at 750 °C (a) and LSCF-900 cathode on YSZ electrolyte sintered at 850 °C (b), and the surface view of LSCF-900 cathode on YSZ electrolyte sintered at 850 °C (c).

ders generally show decreased sintering activity with increasing calcination temperature. It was found that by raising the calcination temperature from 800 to 900 °C (LSCF powders calcined at 900 °C for 5 h will be referred to as LSCF-900 hereafter), the optimal cathode fabrication temperature could be increased to 850 °C and the cathode fabricated at 850 °C using LSCF-

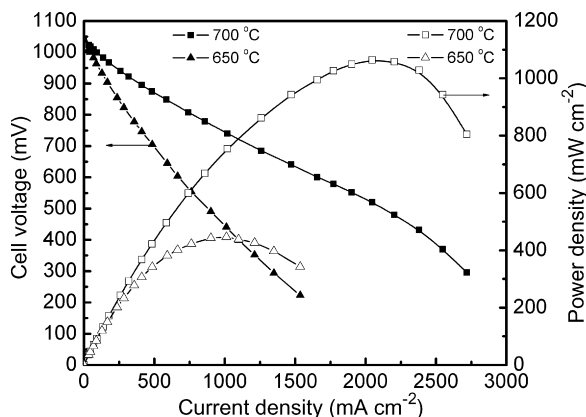


Fig. 8. Cell performance data at operation temperatures of 650 and 700 °C for anode-supported single cell with LSCF-900 cathode sintered at 850 °C for 2 h.

900 showed excellent structure stability at 700 °C, where after being aged for 100 h at 700 °C, significant densification is not observed as illustrated by the cross section and surface view in Fig. 7(b) and (c), respectively. The LSCF-900 cathode sintered at 850 °C also exhibits the highly uniform microstructure with an even distribution of pores and good particle to particle contact, which would be favorable for the cathodic electrochemical reactions.

Fig. 8 shows the I - V performance of an anode-supported single cell Ni-YSZ/YSZ ($\sim 8 \mu\text{m}$)/LSCF-900 with the cathode sintered at 850 °C, measured at 650 and 700 °C. At operation temperature of 650 °C, the maximum power density is 0.45 W cm^{-2} at 1.0 A cm^{-2} and the power density at 0.7 V is about 0.34 W cm^{-2} with current density of 0.50 A cm^{-2} . At operation temperature of 700 °C, the maximum power density is 1.06 W cm^{-2} at 2.0 A cm^{-2} and the power density at 0.7 V is about 0.83 W cm^{-2} with current density of 1.2 A cm^{-2} . Such performances are a little lower than those of the cell with LSCF-800 cathode sintered at 750 °C, due to the decrease of reactive sites resulted from particle growth with the increased sintering temperature. However, the performances achieved on the present single cell are higher than those of anode-supported YSZ cells with interlayer-free LSCF cathode reported previously (0.5 W cm^{-2} at 700 °C and 0.7 V) [11], and can be comparable with the best performance achieved on the Ni-YSZ/YSZ/LSCF cell with CGO interlayer (0.9 W cm^{-2} at 700 °C and 0.7 V) [13]. The good performance obtained in the present study can be attributed to the well adherence of YSZ/LSCF interface, the excellent cathode microstructure and the thin electrolyte film with thickness of only $\sim 8 \mu\text{m}$. Furthermore, it is noted that there is no obvious decrease in the generation performance for the single cell Ni-YSZ/YSZ/LSCF-900 after aging at 700 °C for 100 h, suggesting that LSCF-900 cathode possesses good microstructure stability.

This study indicates that LSCF-900 sintered at 850 °C is suitable to be used as a high-performance cathode material for zirconia-based IT-SOFCs without the CGO interlayer. The sintering activity of LSCF cathode can be tailored through the control of the calcination temperature of the precursor powder,

thus good cell performance and structure stability are achieved on the Ni-YSZ/YSZ/LSCF cells. This interlayer-free design is beneficial to simplify the cell structure and the manufacturing process.

4. Conclusions

- (1) Nanocrystalline $\text{La}_{0.6}\text{Sr}_{0.4}\text{Co}_{0.2}\text{Fe}_{0.8}\text{O}_{3-\delta}$ (LSCF) powder with single perovskite phase was prepared by a nitrate-glycine solution combustion method. The LSCF powder calcined at 800 °C for 5 h and subsequent milled at 760 rpm for 24 h (LSCF-800) has a specific surface area of $22.9 \text{ m}^2 \text{ g}^{-1}$ and an average particle size of 175 nm.
- (2) The LSCF-800 powder possesses high sintering activity, and can be well adhered to YSZ electrolyte after sintering above 700 °C. The best power generation performance of single cell of Ni-YSZ/YSZ/LSCF-800 has been achieved with the LSCF-800 sintered at 750 °C, with peak-power of 507 mW cm^{-2} at 650 °C and 1114 mW cm^{-2} at 700 °C, respectively. On the other hand, the cathode manufactured at 750 °C will be gradually sintered to dense structure due to the good sintering activity under long term operation, resulting in the degradation of cell performance.
- (3) The sintering activity of LSCF cathode can be tailored through altering the calcination temperature of the precursor powder. The optimum sintering temperature of the cathode can be increased to 850 °C by raising the precalcination temperature from 800 to 900 °C. The single cell with this cathode demonstrates good structure stability and high generation performance with the peak-power (W cm^{-2})/power (W cm^{-2}) at 0.7 V of $0.45/0.34$ at 650 °C and $1.06/0.83$ at 700 °C, respectively.
- (4) Excellent power generation performance achieved in the study is ascribed to the cathode with highly uniform microstructure and sufficient adherence to the thin YSZ electrolyte.

Acknowledgement

The financial support from National Natural Science Foundation of China (Grant No. 20221603) is acknowledged.

References

- [1] B.C.H. Steel, A. Heinzl, Nature 414 (2001) 345–352.
- [2] K. Yamahara, C.P. Jacobson, S.J. Visco, X.F. Zhang, L.C.D. Jonghe, Solid State Ionics 176 (2005) 275–279.
- [3] Z.W. Wang, M.J. Cheng, Y.L. Dong, M. Zhang, H.M. Zhang, J. Power Sources 156 (2006) 306–310.
- [4] Y. Mizutani, K. Hisada, K. Ukai, H. Sumi, M. Yokoyama, Y. Nakamura, O. Yamamoto, J. Alloys Compd. 408–412 (2006) 518–524.
- [5] S.P. Yoon, J. Han, S.W. Nam, T.H. Lim, I.H. Oh, S.A. Hong, Y.S. Yoo, H.C. Lim, J. Power Sources 106 (2002) 160–166.
- [6] J.D. Zhang, Y. Ji, H.B. Gao, T.M. He, J. Liu, J. Alloys Compd. 395 (2005) 322–325.
- [7] E.P. Murray, M.J. Sever, S.A. Barnett, Solid State Ionics 148 (2002) 27–34.
- [8] H.Y. Tu, Y. Takeda, N. Imanishi, O. Yamamoto, Solid State Ionics 117 (1999) 277–281.

- [9] A. Mai, V.A.C. Haanappel, S. Uhlenbruck, F. Tietz, D. Stöver, *Solid State Ionics* 176 (2005) 1341–1350.
- [10] F. Tietz, V.A.C. Haanappel, A. Mai, J. Mertens, D. Stöver, *J. Power Sources* 156 (2006) 20–22.
- [11] K. Murata, T. Fukui, H. Abe, M. Naito, K. Nogi, *J. Power Sources* 145 (2005) 257–261.
- [12] H. Klug, L. Alexander, *X-ray Diffraction Procedures for Polycrystalline and Amorphous Materials.*, John Wiley and Sons, New York, 1974, pp. 618–708.
- [13] A. Mai, V.A.C. Haanappel, F. Tietz, D. Stöver, *Solid State Ionics*, in press.
- [14] H.Y. Jung, W.S. Kim, S.H. Choi, H.C. Kim, J. Kim, H.W. Lee, J.H. Lee, *J. Power Sources* 155 (2006) 145–151.